



**Queensland University of Technology**  
Brisbane Australia

This is the author's version of a work that was submitted/accepted for publication in the following source:

Ristovski, Zoran, Surawski, Nicholas C., Miljevic, Branka, Stevanovic, Svetlana, Ayoko, Godwin A., Elbagir, Sohair, Fairfull-Smith, Kathryn E., & Bottle, Steven  
(2011)

On the influence of biodiesel feedstock on compression ignition particulate emissions. In  
*20th Clean Air Society of Australia and New Zealand Conference*, 5-8 July 2011, Christchurch, New Zealand.

This file was downloaded from: <https://eprints.qut.edu.au/108801/>

© 2011 [Please consult the author]

**Notice:** *Changes introduced as a result of publishing processes such as copy-editing and formatting may not be reflected in this document. For a definitive version of this work, please refer to the published source:*

# ON THE INFLUENCE OF BIODIESEL FEEDSTOCK ON DIESEL PARTICULATE EMISSIONS

20<sup>th</sup> ANNUAL CASANZ CONFERENCE, CHRISTCHURCH, 2011

Zoran D. Ristovski<sup>1</sup>, Nicholas C. Surawski<sup>1,2</sup>, Branka Miljevic<sup>1</sup>, Svetlana Stevanovic<sup>1,3</sup>, G.A. Ayoko<sup>4</sup>, Sohair Elbagir<sup>4</sup>, Kathryn E. Fairfull-Smith<sup>3</sup> and Steven E. Bottle<sup>3,4</sup>.

<sup>1</sup>International Laboratory for Air Quality and Health, Queensland University of Technology, 2 George St, Brisbane QLD 4001, Australia

<sup>2</sup>School of Engineering Systems, Queensland University of Technology, 2 George St, Brisbane QLD 4001, Australia

<sup>3</sup>ARC Centre of Excellence for Free Radical Chemistry and Biotechnology, Queensland University of Technology, 2 George St, 4001 Brisbane, Australia

<sup>4</sup>Discipline of Chemistry, Faculty of Science and Technology, Queensland University of Technology, 2 George St, Brisbane QLD 4001, Australia

## Abstract

Particulate emissions from compression ignition engines are a major health concern, especially in underground mine environments where limited ventilation during the operation of diesel powered equipment can exacerbate the problem. Clearly strategies are required to address the diesel particulate matter problem, with alternative fuels, such as biodiesel, having been recently considered to ameliorate the problem. This study considers a physico-chemical characterisation of particulate emissions from an underground coal mine compression ignition engine to determine the effect of using 3 biodiesel feedstocks at 4 different blend percentages. Particle physical properties measured included particle number size distributions and the lung deposited surface area, and particle chemical properties measured included particle and vapour phase polycyclic aromatic hydrocarbons (PAHs) and also the measurement of reactive oxygen species (ROS), which are believed to play an important role in the human body's inflammatory response after exposure to diesel emissions. The particle number size distributions showed strong dependency on both feedstock and the blend percentage employed, with the canola feedstock yielding higher particle number emissions than diesel (followed by tallow), whereas the soy feedstock showed significant particle number reductions. Both particle and vapour phase PAHs were generally reduced with biodiesel, although the results did not exhibit dependence on blend percentage. The ROS concentrations increased monotonically with biodiesel blend percentage but the data did not suggest strong feedstock dependency. It was also shown that ROS emissions correlate quite well with the organic volume percentage of particles which was calculated using unheated and heated particle volume distributions. Whilst biodiesel fuels might be effective at reducing particle mass emissions, some feedstocks increase the number of particles emitted, and all feedstocks increase the oxidative capacity of particles and also emit particles that have a much smaller median diameter than ultra-low sulphur diesel.

*Keywords:* Compression ignition engine, particle emissions, polycyclic aromatic hydrocarbons, reactive oxygen species.

## 1. Introduction

In the underground mining sector, long term exposure to combustion aerosols occurs because of the prevalent usage of equipment powered by compression ignition engines (Bugarski et al., 2009). In an underground mine environment, the emissions occur in a confined space with very little dilution, a process which would act to exacerbate the already known impacts of DPM. This is especially the case considering that dilution conditions have a strong impact on gas-to-particle partitioning of organic aerosol, with a much higher organic aerosol loading being observed when dilution is limited (Robinson et al., 2007). Organic aerosol emissions would include compounds deleterious to human health such as polycyclic aromatic hydrocarbons (PAHs) and reactive oxygen species (ROS) (Sklorz et al., 2007). Clearly, strategies need to be invoked to limit worker exposure to DPM in confined underground mine environments.

One obvious solution to mitigate particulate emissions in the underground mine environment is to filter the exhaust stream using a diesel particulate filter (DPF). In Australia, however, the exhaust of engines that are approved for use in underground coal mines must be mounted in a specially designed water jacket (Standards Australia, 2008) to alleviate the potential combustion hazard due to the presence of methane gas. The prospect of an increased combustion hazard does not make the DPF filtration technique viable, as a high exhaust temperature ( $> 250$  °C if using  $\text{NO}_2$  as an oxidant) is required for the regeneration to work (Dieselnet, 2005). Taking this approach (ie DPF filtration with  $\text{NO}_2$  regeneration) would violate existing Australian standards (exhaust temperature  $< 150$  °C), consequently, other approaches must be explored to achieve the required reductions in DPM emissions.

In this study, a variety of biodiesel feedstocks and blend percentages have been investigated to explore their impact on the physico-chemical properties of diesel particulate emissions. Particle physical properties are addressed by measuring particle number size distributions and chemical properties are addressed by measuring the emissions of PAHs and ROS.

## 2. Methodology

### 2.1. Engine and fuel details

#### 2.1.1. Engine details

Particulate emissions testing was performed on a naturally aspirated 4 cylinder Perkins 1104C-44 engine with a Euro II (off-road) emissions certification. Since Australian underground coal mines currently use this type of engine; the engine selection can be considered representative of the fleet being used in underground mine environments. The engine was coupled to a Heenan & Froude water brake dynamometer (DPX 4) to provide a load to the engine.

#### 2.1.2. Fuel details

In addition to ultra-low sulphur diesel ( $< 10$  ppm sulphur), three biodiesel feedstocks; namely, soy, tallow and canola were tested at four blend percentages (20%, 40%, 60% and 80%). Various fuel blends are denoted by "BX", which means that X % of the total fuel volume is derived from a particular biodiesel feedstock. The biodiesel feedstocks selected are those most relevant from an Australian perspective, as all three feedstocks were commercially available at the time the study was undertaken. The opportunity also arose to test neat soy biodiesel (ie 100% soy), yielding fourteen different fuel types, all of which were tested at the intermediate speed (1400 revolutions per minute) full load (300 Nm) setting for this engine - a test mode known as rated torque. The most representative test mode was pre-selected from the full 13 mode AS3584 test cycle so that the impacts of biodiesel feedstock and blend percentage on the physico-chemical characteristics of particulate emissions (relative to ultra-low sulphur diesel) could be explored in sufficient detail.

### 2.2. Particulates measurement methodology

#### 2.2.1. Measurement overview

The experimental methodology involves diluting a small proportion of the exhaust ( $\sim 1\%$  by volume), followed by a comprehensive analysis of the physico-chemical characteristics of biodiesel and diesel particulate emissions with a range of on and off line aerosol instrumentation and analytical techniques. Dilution of the exhaust gas is performed to reduce the temperature and concentration of particulate matter to a level suitable for aerosol instrumentation, and by doing so, to "mimic" the atmospheric dilution process which naturally takes place as the exhaust plume is emitted from the tail-pipe of an engine.

#### 2.2.2. Dilution system details

A two-stage unheated system was used to dilute the exhaust before particulate measurement; consisting of a dilution tunnel followed thereafter by a Dekati ejector diluter.  $\text{CO}_2$  was used as tracer gas to calculate dilution ratios (Sable Systems Inc  $\text{CO}_2$  analyser), with dilution ratios varying from 165-260 during tests.

### 2.2.3. Off-line chemical measurements

From the dilution tunnel, filter sampling was performed for particle phase PAHs and XAD-2 resin was used to sample vapour phase PAHs. Aerosol was also bubbled through impingers (a test impinger, and a HEPA filtered control filter) containing 20 ml of 4  $\mu\text{M}$  BPEAnit solution, using dimethylsulphoxide (DMSO) as a solvent, followed thereafter by fluorescence measurements of the test and control solutions, to assess the *in vitro* oxidative capacity of particulate emissions, hereafter referred to as ROS concentrations. To quantify ROS emissions, the control fluorescence (ie gas phase species) was subtracted from the test sample fluorescence (ie gas and particle phase species) and a calibration curve relating fluorescence to the amount of fluorescent product (nmol) was used to estimate particle-related ROS concentrations. The amount of fluorescent product was normalised to the particulate mass (measured by a TSI 8520 Dust-trak) to give ROS concentrations in units of nmol/mg of particulate matter. More details on the ROS sampling and quantification methodology such as: the impinger collection efficiency, nitroxide probe theory and its application to various combustion sources can be found in Miljevic et al (2009) and Miljevic et al . (2010a, Miljevic et al., 2010b). Sampling was conducted from the dilution tunnel for the off-line chemical analyses undertaken for this study (ie for PAHs and ROS), to enable sufficiently high concentrations for these analytical techniques to succeed.

### 2.2.4. On line physical measurements

Particle number size distributions were measured with a scanning mobility particle sizer (SMPS) to explore the impact of biodiesel feedstock and blend percentages on the number and size of particles emitted. The SMPS consisted of a TSI 3071A classifier and a TSI 3010 CPC. A TSI 3550 Nanoparticle Surface Area Monitor (NSAM) was used to measure the lung deposited surface area (tracheo-bronchial) emitted by the engine. Size distributions were also passed through a TSI 3065 thermodenuder, which consists of a short heated section (set to 300 °C) followed by an annular bed of activated charcoal to adsorb evaporated material, which in diesel exhaust will be primarily organic in nature. Heating the particles enabled the impact of thermal treatment to be explored. It was hypothesised, *a priori*, that biodiesel could lead to more “volatile” (ie evaporation of organic material) particles, since on a mass basis biodiesel tends to reduce the elemental carbon fraction of particles, whilst an increase in the soluble organic fraction is usually observed. A thermodenuder loss correction was performed using dried NaCl particles.

Figure 1 provides a schematic overview of the experimental methodology used in this investigation.

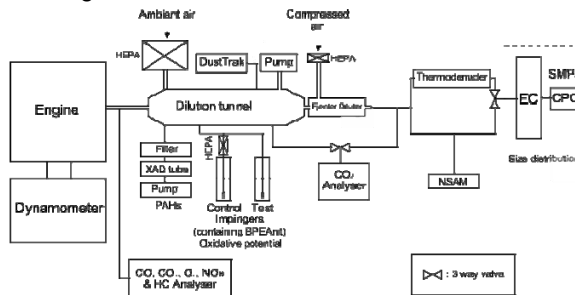


Figure 1. Experimental set-up for this study.

## 2.3. Data analysis

### 2.3.1. Emissions data calculations

All size distributions have been corrected for the total dilution ratio to provide raw exhaust, rather than diluted, concentrations. Particle and vapour phase PAHs are calculated as raw exhaust emissions factors (mg/kWh), hence, being corrected for the primary dilution ratio. ROS concentrations are normalised by mass of particulate matter to give units of nmol/mg (ie nmol of fluorescent product per mg of particulate matter) measured from the dilution tunnel.

### 2.3.2. Particle organic volume percentage calculation

The NSAM surface area data has been converted from a lung deposited surface area to a raw surface area by multiplying by the reciprocal of the tracheo-bronchial deposition efficiency at 80 nm based on the 1994 ICRP model (The International Commission on Radiological Protection, 1994).

The organic volume percentage of particles has been calculated (assuming spherical particles) according to the following formula:

$$V_{org} = 100 \times \left( \frac{\delta}{CMD} \right)^3$$

where:  $V_{org}$  is the volume percentage of the particle that is organic, the  $CMD$  is the count median diameter of the particle number size distributions, and  $\delta$  is the thickness of the organic coating on the surface of the particles.

The organic layer thickness, coating particles, was calculated from particle volume size distributions via:

$$\delta = \left( \frac{V_{unheated} + V_{heated}}{S_A} \right)$$

where:  $V_{unheated}$  is the particle volume for the unheated particles,  $V_{heated}$  is the particle volume for particles heated to 300 °C by the thermo-denuder, whilst  $S_A$  is the “raw” particle surface (ie not lung-deposited), corrected for the total dilution ratio.

### 3. Results and discussion

#### 3.1. Appendicial material

Due to the space constraints placed upon this manuscript, two supplementary Figures and a Table can be found in the Appendix of this manuscript. The appendix contains graphs of the PM<sub>10</sub> emissions (Figure A1) and the count median diameter of particles (Figure A2) as well as calculations for the organic layer thickness ( $\delta$ ) (Table A1).

#### 3.2. Particle number emissions

Figure 2 shows the brake-specific particle number emission factors for all 14 fuel settings. The results show a strong dependency on both biodiesel feedstock and blend percentage. For the soy feedstock, particle number reductions range from 4% (B40) to 53% (B100), whilst for B20 a 12% particle number increase occurs. Particle number increases range from 71% (B20) to 44% (B80) for the canola feedstock. For the tallow feedstock, particle number increases range from 7% (B20) to 25% (B40), whilst a particle number reduction of 14% occurs for B80.

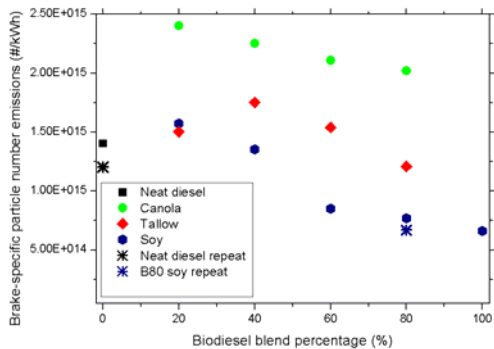


Figure 2. Brake-specific particle number emission factors (#/kWh) for various biodiesel feedstocks and blend percentages.

It is interesting to note that non-monotonic trends in the particle number emissions were observed for all 3 feedstocks. Non-monotonic particle number emissions with increasing blend percentages were observed by Di et al. (2010) and the complex oxidation behaviour of biodiesel particle emissions

was implicated in this phenomenon. Given the absence of combustion-related diagnostic data, it is quite difficult to provide a detailed mechanistic description of this result at this stage.

#### 3.3. Particle number size distributions

Panels 1-4 from Figure 3 show particle number size distributions for the 3 biodiesel feedstocks and 4 blend percentages. The shift to a smaller median particle diameter can also be readily observed as the blend percentage is increased, and does so in a monotonic fashion. This is of particular concern considering that smaller particles have a much higher likelihood of deposition in the alveolar region of the lung (The International Commission on Radiological Protection, 1994). The canola feedstock produced particles with the smallest median size, followed by tallow and then the soy feedstock. A somewhat concerning result is that the feedstock that produces the most particles (ie canola) also produces the smallest particles.

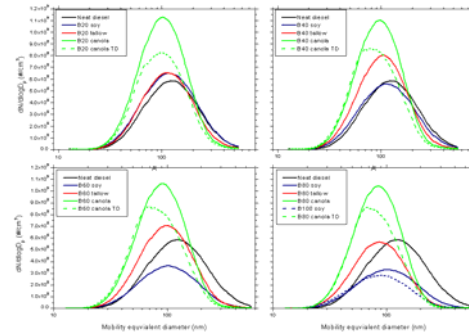


Figure 3. Particle number size distributions for various biodiesel feedstocks and blend percentages.

Size distributions are also shown in Figure 3 where the poly-disperse size distribution was passed through a thermodenuder set to 300 °C for the canola feedstock. The canola feedstock was chosen to illustrate the “volatility” of particles, as they had the highest organic content, subsequently exhibiting significant evaporation in a thermodenuder. It can be observed that organic compounds (such as PAHs and ROS) are “internally mixed” on the particle surface, as heating the particles has not introduced a secondary peak in the resulting size distribution.

#### 3.4. PAH emissions

Figure 4 shows the particle (top panel) and vapour (bottom panel) phase PAH emissions. Although some data points conspire to prevent universal trends in the data set (eg the diesel and B80 soy repeat tests are not consistent), it is readily apparent that both particle and vapour phase PAHs are reduced by biodiesel. It should be noted

though that the dependence on blend percentage is not of a monotonic nature, a finding consistent with the results of Ballesteros et al (2010). According to the USEPA (United States Environmental Protection Agency, 2002), PAH emissions tend to correlate with the gaseous hydrocarbon emissions emitted by a compression ignition engine. Given that hydrocarbon emissions are usually reduced with biodiesel (Lapuerta et al., 2008), this offers a tentative explanation for the PAH results observed in this investigation.

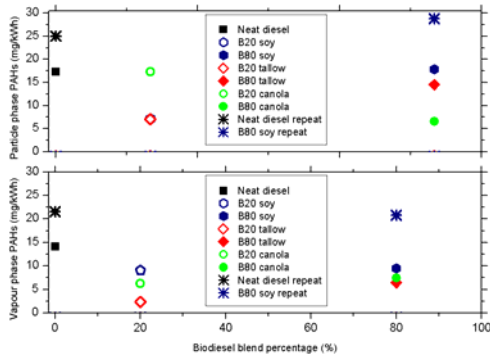


Figure 4. Particle and vapour phase PAH emissions for various biodiesel feedstock and blend percentages.

### 3.5. ROS concentrations

Alternatively, the ROS concentrations (where a successful fluorescence signal was observed) increase in a monotonic fashion with biodiesel blend percentage (Figure 5). Cheung et al (2009) observed an increase in the production rate of superoxide ions ( $O_2^-$ ) on a mass basis with the use of neat soy biodiesel. Furthermore, the ROS results show less feedstock variability than the results presented thus far. In terms of the chemical mechanism leading to an increase in ROS concentrations, it is believed that oxygenated fuels (such as biodiesel) emit more OH radicals (Kitamura et al., 2001). OH radicals have the potential to react with DMSO creating methyl radicals ( $CH_3$ ) which are trapped by the nitroxide probe leading to a greater fluorescence signal.

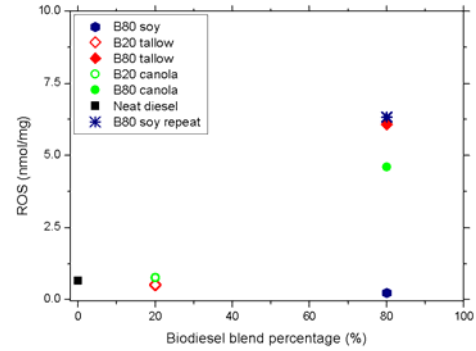


Figure 5. ROS concentrations for various biodiesel feedstock and blend percentages.

### 3.6. ROS organic volume correlation

ROS are generally classed as “semi-volatile” organic compounds that evaporate when exposed to thermal treatment with a thermo-denuder (Miljevic et al., 2010b). It therefore seems intuitive to seek a correlation between ROS concentrations and the volume percentage of the particle that is composed of organic material. The results in Figure 6 represent an attempt to establish this correlation. In general, higher ROS emissions are associated with particles that have a greater organic volume percentage, although the B80 tallow data point is a notable exception. Despite one potential outlying data-point, the Pearson correlation co-efficient for this relationship is quite strong ( $\sim 0.83$ ). It can be observed from this graph that as biodiesel blend percentage is increased; the particles are internally mixed with more ROS and also have a higher organic content.

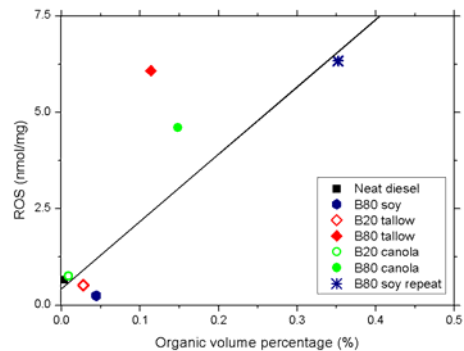


Figure 6. The relationship between the organic volume percentage of particles and their ROS concentrations for various biodiesel feedstocks and blend percentages.

## 4. Conclusions

The results show that whilst significant particle mass reductions are achieved with all 3 biodiesel feedstocks (Figure A1), unregulated particulate

emissions, such as particle number concentration and ROS concentrations are increased by some and all feedstocks, respectively.

The results from this study have shown strong dependence of the physico-chemistry of biodiesel particles on both biodiesel feedstock, but also blend percentage. As a result, it does not appear that results from testing a particular feedstock can be "generalised" to other biodiesel feedstocks. Furthermore, the results from this study show that the physico-chemical properties of the particles do not necessarily follow monotonic trends with respect to blend percentage. Consequently, to properly characterise the impact of biodiesel fuels on particulate emissions, different feedstocks and blend percentages should be tested on an individual basis.

### Acknowledgements

The authors wish to acknowledge support and funding provided by SkillPro Services Pty Ltd and the Australian Coal Association Research Program for funding project C18014. Special thanks go to Mr Julian Greenwood and Mr Dale Howard, from SkillPro Services, for their technical expertise throughout testing, and also for operating the dynamometer and providing the gaseous emissions and diagnostic test data.

### References

- Ballesteros, R., Hernandez, J. J. & Lyons, L. L. (2010) An experimental study of the influence of biofuel origin on particle-associated PAH emissions. *Atmospheric Environment*, 44, 930-938.
- Bugarski, A. D., Schnakenberg, G. H., Hummer, J. A., Cauda, E., Janisko, S. J. & Patts, L. D. (2009) Effects of Diesel Exhaust Aftertreatment Devices on Concentrations and Size Distribution of Aerosols in Underground Mine Air. *Environmental Science & Technology*, 43, 6737-6743.
- Cheung, K. L., Polidori, A., Ntziachristos, L., Tzamkiozis, T., Samaras, Z., Cassee, F. R., Gerlofs, M. & Sioutas, C. (2009) Chemical Characteristics and Oxidative Potential of Particulate Matter Emissions from Gasoline, Diesel, and Biodiesel Cars. *Environmental Science & Technology*, 43, 6334-6340.
- Di, Y., Cheung, C. S. & Huang, Z. H. (2010) Experimental investigation of particulate emissions from a diesel engine fueled with ultralow-sulfur diesel fuel blended with diglyme. *Atmospheric Environment*, 44, 55-63.
- Dieselnet (2005) Diesel Filter Regeneration. Dieselnet technology guide, Ecopoint Inc, [http://www.dieselnet.com/tech/dfp\\_regen.html](http://www.dieselnet.com/tech/dfp_regen.html).
- Kitamura, T., Ito, T., Senda, J. & Fujimoto, H. (2001) Extraction of the suppression effects of oxygenated fuels on soot formation using a detailed chemical kinetic model. *Society of Automotive Engineers of Japan*, 22, 139-145.
- Lapuerta, M., Armas, O. & Rodriguez-Fernandez, J. (2008) Effect of biodiesel fuels on diesel engine emissions. *Progress in Energy and Combustion Science*, 34, 198-223.
- Miljevic, B., Fairfull-Smith, K. E., Bottle, S. E. & Ristovski, Z. D. (2010a) The application of profluorescent nitroxides to detect reactive oxygen species derived from combustion-generated particulate matter: Cigarette smoke - A case study. *Atmospheric Environment*, 44, 2224-2230.
- Miljevic, B., Heringa, M. F., Keller, A., Meyer, N. K., Good, J., Lauber, A., Decarlo, P. F., Fairfull-Smith, K. E., Nussbaumer, T., Burtscher, H., Prevot, A. S. H., Baltensperger, U., Bottle, S. E. & Ristovski, Z. D. (2010b) Oxidative Potential of Logwood and Pellet Burning Particles Assessed by a Novel Profluorescent Nitroxide Probe. *Environmental Science & Technology*, 44, 6601-6607.
- Miljevic, B., Modini, R. L., Bottle, S. E. & Ristovski, Z. D. (2009) On the efficiency of impingers with fritted nozzle tip for collection of ultrafine particles. *Atmospheric Environment*, 43, 1372-1376.
- Robinson, A. L., Donahue, N. M., Shrivastava, M. K., Weitkamp, E. A., Sage, A. M., Grieshop, A. P., Lane, T. E., Pierce, J. R. & Pandis, S. N. (2007) Rethinking organic aerosols: Semivolatile emissions and photochemical aging. *Science*, 315, 1259-1262.
- Sklorz, M., Briede, J. J., Schnelle-Kreis, J., Liu, Y., Cyrys, J., De Kok, T. M. & Zimmermann, R. (2007) Concentration of oxygenated polycyclic aromatic hydrocarbons and oxygen free radical formation from urban particulate matter. *Journal of Toxicology and Environmental Health-Part a-Current Issues*, 70, 1866-1869.
- The International Commission on Radiological Protection (1994) *Human respiratory tract model for radiological protection*, ICRP publication 66, Oxford, Elsevier Science Ltd.
- United States Environmental Protection Agency (2002) A comprehensive analysis of biodiesel impacts on exhaust emissions. Draft technical report, pp 1-126.

## 5. Appendix

Two Figures and a Table constitute the appendicial material for this manuscript.

B80 canola	8.07E+13	9.5
B80 soy repeat	6.64E+13	14.9

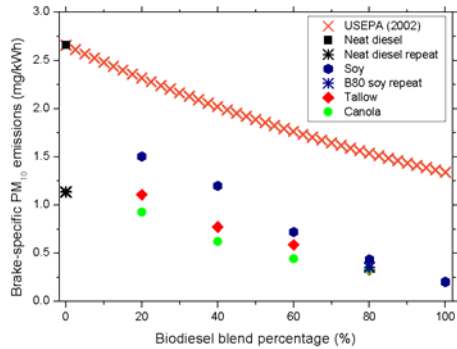


Figure A1: Brake-specific PM<sub>10</sub> emissions (mg/kWh) for various biodiesel feedstocks and blend percentages. Note that the USEPA (2002) trend-line is included for comparison.

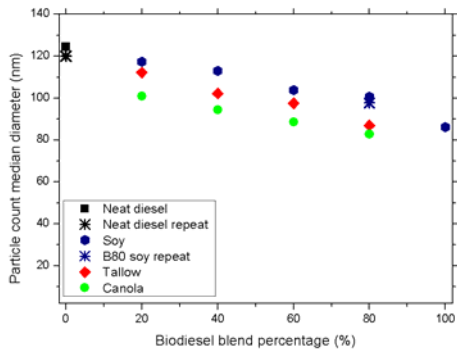


Figure A2: Count median diameters (nm) from the particle number size distributions for various biodiesel feedstocks and blend percentages.

Table A1: Volatile volume and organic layer thickness calculations for various biodiesel feedstocks and blend percentages.

Fuel setting	Volatile Volume (nm <sup>3</sup> /cm <sup>3</sup> )	Organic layer thickness (δ) (nm)
Neat diesel	9.05E+13	4.0
B20 soy	2.60E+14	16.4
B80 soy	5.22E+13	7.7
B20 tallow	7.52E+13	7.3
B80 tallow	5.62E+13	9.1
B20 canola	5.41E+13	4.5